# Low-temperature recombination kinetics of photoexcited persistent charge carriers in conjugated polymer/fullerene composite films

N. A. Schultz, M. C. Scharber, C. J. Brabec, and N. S. Sariciftci
*Linz Institute for Organic Solar Cells (LIOS), Physical Chemistry, Johannes Kepler University of Linz, Altenbergerstr. 69, A-4040 Linz, Austria*

(Received 13 June 2001; published 6 December 2001)

The recombination kinetics of long-lived photoexcited charge carriers in a composite of poly[2-methoxy-5-(3′,7′-dimethyloctyloxy)-1,4-phenylene vinylene] (MDMO-PPV) and 1-(3-methoxycarbonyl)-propyl-1-phenyl-(6,6)$C_{61}$ (PCBM) at low temperatures ($T=40$ K) are investigated by light induced electron-spin resonance (LESR). These long-lived (persistent) photoinduced charge carriers exhibit recombination times that extend over several hours after cessation of the photoexcitation. These long relaxation times can be explained by nongeminate recombination of randomly distributed carriers assuming charge neutrality. The decay curves fit well to a model in which the recombination mechanism of photoexcited carriers consists of tunneling processes and in which the recombination rate only depends on the intrapair distance between the photoexcited carriers. It is shown that the residual photoexcited carrier concentration after long times tends to be independent of the generation rate. The presented model has already been successful in describing the recombination kinetics of photoexcited carriers in inorganic, amorphous semiconductors, which indicates that the presented recombination mechanism is common to disordered organic and inorganic materials.

DOI: 10.1103/PhysRevB.64.245210 PACS number(s): 72.20.Jv, 72.80.Le, 72.80.Ng, 67.30.−v

## I. INTRODUCTION

The understanding of electronic processes, such as photoexcitation and recombination of charge carriers in conjugated polymers is of fundamental interest for both material characterization and device fabrication. In particular, the addition of fullerenes, e.g., $C_{60}$, into the conjugated polymer, leads to charge separation on a 10-femtosecond time scale after photoexcitation.[1–3] The back transfer occurs on the order of microseconds (at room temperature), thus creating an intrinsic asymmetry between forward and back electron transfer of over eight orders of magnitude.[3,4] The observation of persistent photoexcited carriers with lifetimes that exceed even hours at low temperatures ($T<100-200$ K) apparently complicates the understanding of the recombination mechanism.[5] These very long-lived photoexcited carriers have already been observed with several techniques. In electron-spin resonance (ESR) a light induced signal is observed to decrease over several hours after cessation of the photoexcitation.[5] Interestingly, also the increase of the light induced ESR (LESR) signal, i.e., an increase in the number of photoexcited carriers, can be observed for several hours, when the intensity of the photoexcitation is sufficiently low. Both the extremely slow accumulation of long-lived carriers and their long-time decay are also seen in a polydiacetylene[6] with the technique of photoinduced absorption (PIA) as a long rise and decay of photoexcited carriers that extends over several minutes. From PIA-Fourier transform infrared (FTIR) measurements it was concluded that the long-lived photoexcitations are (spin-$\frac{1}{2}$) polaronlike, massive (300 $m_e$) defects.[7]

Photoexcited, long-lived carriers have only been observed at low temperatures. This is most consistent with a picture in which the long-lived carriers are trapped, i.e., localized, below the band edges with trap energies larger than their thermal energy $kT$. At sufficiently high temperatures thermal reexcitation of the trapped carriers, followed by diffusion and enhanced recombination, is the reason why no long-lived carriers are observable at higher temperatures. At higher temperatures the decay of the long-lived carriers as measured by ESR can be well fit to an expression that decreases exponentially in time,[6] indicating a thermally activated behavior. Furthermore, by applying an electric field at low temperatures and slowly increasing the temperature it is possible to observe the drift of the reexcited carriers, i.e., the current, and to get information on the trapping depth.[8–10] It has also been shown that the long-lived carriers can optically be reexcited and detected by their current in an applied field.[8] Interestingly, long-lived photoexcited carriers with a similar experimental finger print as those reported here have also been observed in disordered, inorganic materials, such as hydrogenated amorphous silicon ($a$-Si:H) and germanium ($a$-Ge:H).[11] In these materials long-lived carriers recombine at temperatures above approximately 150 K and can also be optically induced to recombine.[11,12]

In this work the very long-lived photoexcited charge carriers in a conjugated polymer/fullerene composite are examined and the results are explained on the basis of a theoretical model involving distance dependent recombination kinetics that has already been successful in describing the long lifetimes of photoexcited carrier at low temperatures in inorganic semiconductors.[11]

## II. EXPERIMENT

The conjugated polymer used for the current studies was poly[2-methoxy-5-(3′,7′-dimethyloctyloxy)-1,4-phenylene vinylene], denoted as MDMO-PPV, and was supplied by Covion. 1-(3-methoxycarbonyl)-propyl-1-phenyl-(6,6)$C_{61}$ [PCBM],[13] a highly soluble methanofullerene, was dissolved

 

with MDMO-PPV in toluene. A composite of MDMO-PPV/PCBM ((10±1)% PCBM by weight) was deposited by the doctor blading technique onto a plastic substrate. This concentration corresponds to about 1 PCBM molecule per 30 polymer repeating units. Fifteen pieces, each with an approximate size of 1.5 mm×2 cm, were cut from the substrate and put into an ESR grade quartz tube and sealed in helium atmosphere. The thickness of the composite film, which also varies over the 15 pieces, was estimated to be in the range from 0.2 to 0.5 $\mu$m. For the ESR measurements a Bruker EMX spectrometer ($X$ band) with an Oxford variable temperature cryostat that controlled the sample temperature between 4 and 300 K with an accuracy of approximately 0.1 K was used. All measurements were performed at 40 K, except where noted otherwise. The sample was excited by an $Ar^+$ laser (476 nm) through an optical fiber that terminated at the quartz tube inside the cavity. The exciting light entering the cavity was unfocused and estimated to be at most 0.5 W. From the end of the fiber the light either directly hit the sample or is reflected from the inside cavity walls until it eventually hit the sample to get absorbed. Averaged over the approximate total sample area of about 4.5 $cm^2$ this leads to a maximum light intensity of at most 0.1 $W/cm^2$. However, some light is lost through the optical windows of the cavity lowering this average and, on the other hand, shielding effects among the samples can cause much higher local light intensities. Due to these uncertainties in the light intensity that is actually incident on the sample, only relative light intensities are given. Before each measurement of the long-lived photoexcited carriers the sample was cooled down from room temperature in the dark. This procedure assures that previously excited carriers have completely recombined and no carriers are inadvertently excited during the cooling process.

## III. THEORY

The recombination kinetics of trapped carriers by tunneling processes were considered by Dunstan.[14] Shklovskii and co-workers[15–18] proposed a detailed model that describes these recombination kinetics of the photoexcited carriers at low temperatures. After photoexcitation a carrier pair can either immediately recombine geminately or separate by diffusion. Trapping or other recombination processes follow diffusion. Among these recombination processes it can be assumed that geminate recombination is strongest within short times after photoexcitation, although not immediately afterwards,[16] whereas after longer times nongeminate recombination prevails. These processes will lead to a situation in which eventually all geminate pairs and mobile carriers have recombined and all residual carriers are randomly trapped. This randomness, however, is limited to volumes with an expansion, which is on the order of the diffusion length. In amorphous organic materials like conjugated polymers the mobility of the photoexcited carriers is very low at low temperatures,[19] charge neutrality exists on larger scales. At sufficiently low temperatures, where reexcitation of the trapped carriers is not possible, the only possible fate of these trapped carriers is a recombination processes by tunneling at longer times. Thermal reexcitation of trapped carriers is neglected in the model, i.e., the model is developed for $T=0$ K.

The explicit development of the model used in this report was shown before.[11,20] The basic assumption of the model is that spatially close carriers have a much higher recombination rate than distant carriers. In particular, the recombination rate can be written as

$$\nu(R)=\nu_0 \exp\left(-\frac{2R}{a}\right), \tag{1}$$

where $\nu(R)$ describes the recombination rate of any electron and hole that are separated by a distance $R$. $\nu_0=\tau_0^{-1}$ is a recombination constant that may be interpreted as an attempt to recombine frequency. The parameter $a$ describes an effective localization radius. Electrons and holes are likely to have different localization radii. The localization radius for the electron is probably on the order of the radius of the PCBM molecule. Holes, which are assumed to be trapped as polarons on the polymer chain, are distributed over several monomer units. Since in the examined processes recombination depends on the mutual overlap of the wave functions of electrons and holes, $a$ describes an effective radius. From Eq. (1) it follows that after some time $t$, spatially close carriers will have recombined, thus leaving carriers with larger distances behind. Therefore, by recombination of the closest pairs, the nearest-neighbor distance $R(t)$ increases and can be written as

$$R(t)=\frac{a}{2}\cdot \ln\left(\frac{t}{\tau_0}\right). \tag{2}$$

Now, assuming that the photoexcitation is turned off at some time $t_0=0$ at a charge carrier concentration $n_0$ and taking into account a time period $t_1-t_0$, in which geminate recombination is present, it can be shown[11,20] that for times larger than $t_1$ the remaining concentration of charge carriers $n(t)$ after cessation of the photoexcitation could be written as

$$n(R)=\frac{n_1}{1+\frac{4\pi}{3}n_1(R^3-R_1^3)}, \tag{3}$$

where the time dependence is contained in $R=R(t)$ given by Eq. (2) with $t>t_1$. $R(t)$ describes the increase of the nearest neighbor distance among the remaining electron hole pairs, which have not recombined until the time $t$ after photoexcitation. $R_1=R(t_1)$ describes the nearest-neighbor distance between the electrons and holes at time $t_1$ after which solely nongeminate recombination is assumed. $n_1$ is the charge carrier concentration at time $t_1$. It follows from Eq. (3) that the time dependence of the residual carrier concentration does not follow a simple exponential decay, but shows a more logarithmic time behavior. After very long times, i.e., at large $R$, one obtains from Eq. (3): $n(R)=[(4\pi/3)R^3]^{-1}$, from which follows that the long-time residual carrier concentration is independent of the initial carrier density $n_1$ and also $n_0$. It follows from Eq. (1) together with the logarithmic time dependence of $R(t)$ that some photoexcited carriers

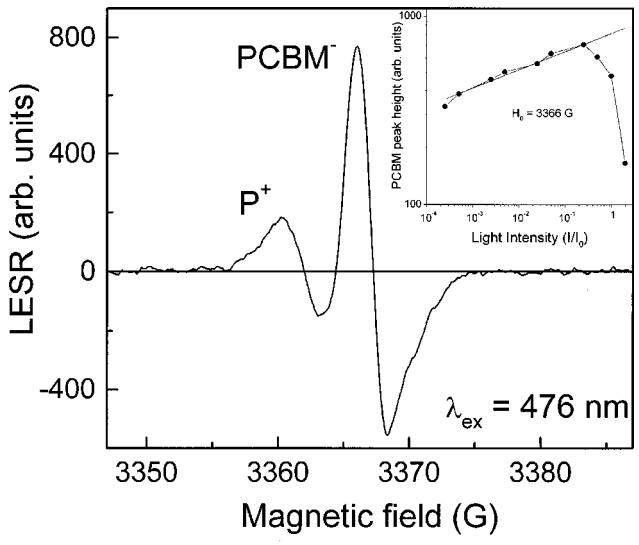


FIG. 1. Light induced electron-spin resonance (LESR) spectrum of MDMO-PPV:PCBM (10%) at 40 K. The resonance is a superposition of at least two individual resonances that are attributed to a lower-field resonance dominantly ascribed to positive polarons $P^+$ and a higher-field narrow resonance ascribed to electrons on the fullerene molecule $PCMB^-$. Inset: The narrow LESR resonance increases as a power law with light intensity $I_{ex}$, according to $LESR \sim I_{ex}^{0.1}$.

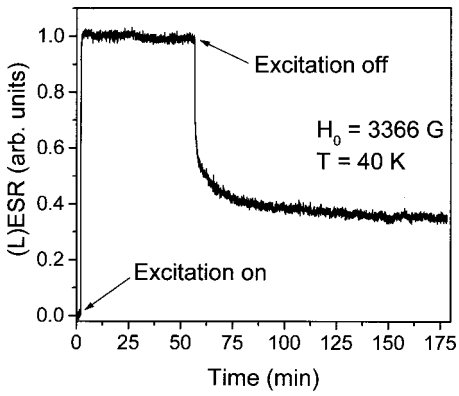


FIG. 2. Rise and decay of the $PCBM^-$ related (L)ESR signal after the photoexcitation has been turned on and off, respectively.

have very long lifetimes, which in this model are solely ascribed to the large distances that build up between the remaining trapped carriers. This picture is in qualitative difference to the previous model,[5] where the observation of long lifetimes was ascribed to carriers localized in deep traps. Note that the parameters in Eq. (3) are all strongly constrained. The excited carrier concentration $n_1$ follows directly from ESR measurements. The localization radius $a$ and the typical radiative lifetimes, $\tau_0 = \nu_0^{-1}$, can either be determined by other measurements or can be guessed in a physically reasonable range. $R_1$ is determined through $t_1$, i.e., the time period after which solely nongeminate recombination can be assumed. No freely adjustable parameters are contained in the model.

## IV. RESULTS

The dark ESR signal in the fullerene doped sample (the composite) was barely detectable at all temperatures. However, under photoexcitation an intense LESR signal as shown in Fig. 1 is found, confirming earlier results.[1,5,21,22] It is attributed to two superimposed signals, where a broader signal at lower magnetic fields is ascribed to positive polarons $P^+$ on the polymer chain and a narrow signal at higher fields is ascribed to electrons on the PCBM, $PCBM^-$. Although it has not been experimentally resolved yet, the broader signal might also contain a small ESR contribution from negative polarons on the polymer chain. In Fig. 1 the electron LESR signal appears to be larger than the polaron LESR signal. We ascribe this observation to the very different saturation behaviors of the two resonances. The polaron LESR signal saturates at much lower microwave powers than the $PCBM^-$ resonance,[5] which was ascribed to the longer spin-lattice relaxation time of the polaron compared to the fullerene anion. The inset of Fig. 1 shows the LESR excitation intensity dependence. For this measurement the magnetic field was fixed to the $PCBM^-$ resonance field and the photoexcitation intensity was stepwise increased. Within three orders of magnitude of excitation intensity $I_{ex}$ the $PCBM^-$ peak of the LESR signal—as measured from the baseline— increases and can be well fit to a power law, $LESR \sim I_{ex}^{\alpha}$, with $\alpha \sim 0.1 \pm 0.02$. Since the narrow, high-field LESR signal is superimposed on the broader low-field LESR signal, its height must actually be measured from the broad LESR line. Since the peak of the positive polaron LESR signal approximately increases with the same power law as the $PCBM^-$ related peak, the photoexcitation intensity dependence of the high-field resonance could be measured from the baseline. Also the other peaks and minima of the LESR spectrum of Fig. 1 are found to follow a power law with exponents close to $\alpha = 0.1$. At very low excitation intensities the LESR carrier concentration does not reach a steady state value within 30 min. of continuous photoexcitation, but slowly keeps increasing for several hours. However, given enough time, the authors expect that also at lowest excitation intensities the LESR signal will follow the observed power law. At very high excitation intensities the LESR signal decreases, which is likely due to sample heating from strong photon absorption. For all measurements reported here the employed laser intensities were in the power-law regime of excitation intensities, thus ruling out any heating effects due to high laser intensities.

Figure 2 shows a typical measurement of the growth and decay of the photoexcited spins at 40 K. The magnetic field was set to the $PCBM^-$ peak of the LESR signal. At time $t = 0$ the spin density corresponds to the dark spin density, which was barely resolved within the noise level. Since only the kinetics of the photoexcited carriers is of interest, the dark spin density is subtracted from the measurement, leading to zero photoexcited carriers at $t = 0$. Then, after about two minutes of measuring the dark spin density, the photoexcitation was turned on and the growth of the LESR signal due to the accumulation of photoexcited carriers on the fullerene molecules was monitored. At the photoexcitation intensity used the LESR signal rapidly increases and reaches a steady state value within one hour. Then, after about 1 h of

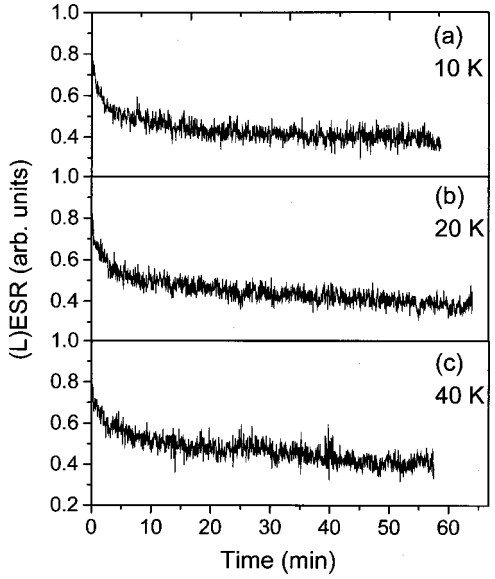


FIG. 3. ESR carrier decay at 10, 20, and 40 K. All data are normalized at $t=0$ and drop off to about 40% within 60 min. No enhanced recombination kinetics due to thermal reexcitation is observed at temperatures $T \leqslant 40$ K.

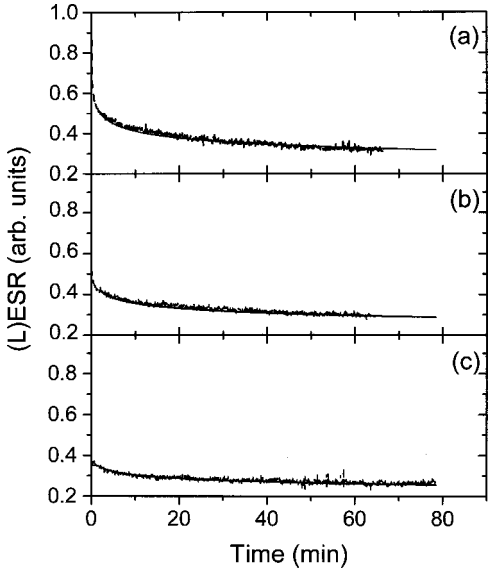


FIG. 4. Carrier decay at 40 K. The relative excitation intensities from top to bottom correspond to $10^{-1}I_0$, $10^{-3}I_0$, and $10^{-4}I_0$, which lead to relative carrier densities $n_1/n_0$ at $t_1=2$ min of (a) 0.5, (b) 0.42, and (c) 0.34, respectively. $I_0$ is at most on the order of 0.1 W/cm$^2$. The solid lines are fits to Eq. (4) for times $t>2$ min with $\tau_0=6\times10^{-5}$ s and $a^3n_0=7\times10^{-4}$.

continuous illumination the excitation was turned off and the decay of the photoexcited carriers in the dark was measured. A rapid decay is followed by a much slower component that is still observable after many hours. Interestingly at sufficiently low excitation intensities an initial rapid LESR increase is followed by a very much slower increase for many hours. In the following only the decay curves such as the one shown in Fig. 2 will be examined.

The presented model is based on photoexcitations followed by thermalization and recombination. However, at actual measurement temperatures $T>0$ K also thermal reexcitation occurs. To examine any thermal effects on the decay curves, three decay curves at 10, 20, and 40 K were recorded. Figure 3 shows these decay curves normalized at the time the photoexcitation was stopped to account for the intrinsic temperature dependence of the ESR signal (Curie law). To avoid microwave saturation of the ESR signal at lowest temperatures, very low microwave intensities were employed. It can be seen that within the first hour after cessation of the photoexcitation, all decay curves show approximately the same decay kinetics. Additionally, the magnetic-field ESR spectrum of the residual carriers were measured immediately following the decay measurements of Fig. 3. For better comparison each of these ESR measurements were done at 40 K. In all three cases the samples showed almost equal residual carrier concentrations, independent of whether the photoexcited carriers had decayed at 10, 20, or 40 K. These results prove temperature-independent recombination kinetics below 40 K and therefore rule out any significant thermal reexcitation at 40 K and lower temperatures. These results are very similar to those reported for $a$-Si:H, where also no thermal reexcitation is observed below 40 K.[20]

Figure 4 shows three decay curves of spin carriers, which had been excited at different photon intensities. The observed short-time spikes in the decay measurements are ascribed to inhomogeneities in the helium flow and therefore to short-time temperature fluctuations. The initial, photoexcited spin concentration at $t=0$ was varied by about a factor of 2, which required a variation of the excitation intensity of about three orders of magnitude (see inset of Fig. 1). The decay measurements of Fig. 4 at three different laser intensities are made at the abscissa values of $10^{-4}$, $10^{-3}$, and $10^{-1}$ of the inset of Fig. 1. These laser intensities assure that the steady-state (SS) LESR signal can be reached (at lower excitation intensities) and that sample heating can be neglected (at higher excitation intensities). Due to the uncertainties in the sample volume that is actually photoexcited and inherent uncertainties of the ESR technique to determine the absolute spin concentration to within a factor of about 2, the authors are not able to determine the absolute concentration of photoexcited spins within reasonable limits. Therefore all decay curves have been normalized by the number of SS-LESR spin carriers $n_0$ at the highest excitation intensity $I_0$ of Fig. 4(a). The solid lines in Fig. 4 are fits to the following equation:

$$\frac{n(t)}{n_0}=\frac{\frac{n_1}{n_0}}{1+\left(\frac{n_1}{n_0}\right)\frac{\pi}{6}n_0a^3\left[\ln^3\left(\frac{t}{\tau_0}\right)-\ln^3\left(\frac{t_1}{\tau_0}\right)\right]} \tag{4}$$

which follows from Eqs. (2) and (3). The ratio $n(t)/n_0$ can directly be read off the graphs of Fig. 4. It can be seen that only the product $a^3n_0$ and the prefactor $\tau_0=\nu_0^{-1}$ enter Eq. (4) as parameters. $t_1=2$ min was chosen to completely avoid effects of geminate recombination at early times during the decay. However, also $t_1=1$ min results in equally good fits. The values for $n(t_1)/n_0=n_1/n_0$ also follow from the graphs

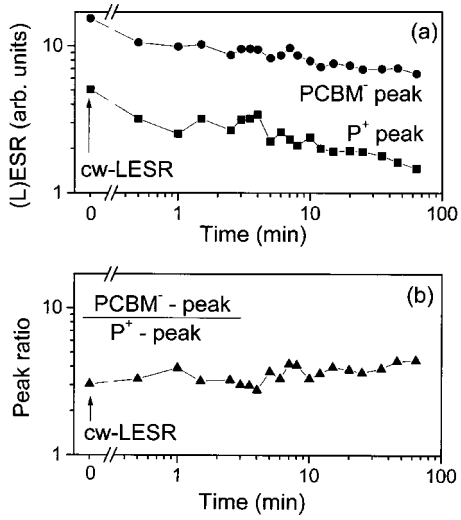


FIG. 5. (a) Decay of the $P^+$ (bullet) and the $PCBM^-$ (square) ESR signals after photoexcitation. The resonances are measured from the ESR baseline. (b) shows the ratio of the resonances in (a), which increases with time $t$ approximately as $t^{0.025}$.

in (a), (b), and (c) and are given by 0.5, 0.42, and 0.34, respectively. For all decays it was found that the slow kinetics of charge carrier recombination could be described with a single set of parameters, namely $\tau_0 = 6 \times 10^{-5}$ s and $n_0 a^3 = 7 \times 10^{-4}$. Note that the fit function, Eq. (4), is only weakly dependent on the value of $\tau_0$ for times much larger than $t_1$, i.e., a variation of $n_0 a^3$ within about 10% can almost be compensated by a corresponding change of $\tau_0$ by about a factor of 10 to result in a similar good fits.

Since the LESR signal of the MDMO-PPV:PCBM is a superposition of at least two resonances, the peak height of the $PCBM^-$ depends on the position of its baseline. This baseline is the polaron related LESR signal that also varies with time. Figure 5(a) compares the decay of the $PCBM^-$ and the $P^+$ related peak after cessation of the photoexcitation. The first data point at $t=0$ reflects the steady-state LESR peak heights under continuous illumination. Then the photoexcitation was turned off and subsequent magnetic-field ESR scans were taken. From these scans the peak heights of the $PCBM^-$ and the $P^+$ signals were plotted as a function of time, where the peak heights are measured from the ESR baseline. It can be seen that both signals decay approximately equally rapid. Figure 5(b) shows the ratio of the peak heights proving that this ratio is almost time independent, which is consistent with the necessity of charge neutrality (always two carriers of opposite polarity recombine, i.e., one carrier from each peak). When the ratio is fitted to a power law in time $\sim t^{\beta}$, $\beta$ is approximately 0.025. This very slow increase can be ascribed to the decay of the underlying $P^+$ ESR signal, which modifies the baseline for the fullerene signal. The overall effect of this baseline shift is that the measured $PCBM^-$ resonance (as also measured in Fig. 4) decays marginally slower than the actual carriers, with the tendency of marginally reducing $\tau_0$ and $a^3 n_0$ in the fit. However, as seen by the very weak time dependence in Fig. 5(b), this effect is extremely small and will be neglected in the following considerations.

## V. DISCUSSION

All decays of Fig. 4 can be well fit with the presented model using a single set of physically constrained parameters and without the use of scaling parameters. However, the prefactor $\nu_0 = (\tau_0)^{-1} = 1.7 \times 10^4\ \mathrm{s}^{-1}$, which may be interpreted as an attempt-to-recombine frequency appears rather small. It translates into a lifetime prefactor of about $6 \times 10^{-5}$ s. In the corresponding measurements of $a$-Si:H a lifetime prefactor of about $1 \times 10^{-8}$ s resulted in good fits.[11] We ascribe the much larger value of the lifetime prefactor in the conducting polymer to enhanced polaronic effects of the holes. In tunneling processes the recombination probability depends on both, the spatial distance among the carriers, i.e., the width of the energy barrier, as well as the height of the energy barrier. The model only considers the spatial distance among carriers, thus the exponential factor containing the energy barrier height must be contained in the prefactor. Due to the formation of polarons in the polymer, the energy barrier height for tunneling is probably higher than in inorganic semiconductors, thus leading to a smaller recombination prefactor. In the following the other parameter, $n_0 a^3 = 7 \times 10^{-4}$, will be discussed. With a better knowledge of the initial spin density $n_0$, it would in principle be possible to calculate the effective localization radius $a$. Assuming the photoexcited electrons of the photoexcited carriers to be localized on the PCBM molecules with a diameter of about 1 nm and the photoexcited holes to be distributed over several monomer units of the polymer a rough estimate of the effective localization radius might be a $\approx$1 nm. With an effective localization radius of about $a \approx 1$ nm an initial spin concentration $n_0$ of roughly $1 \times 10^{18}\ \mathrm{cm}^{-3}$ follows, which is the approximate concentration of PCBM molecules in the sample. Due to the efficient charge transfer of electrons from the polymer to the PCBM molecules it can be assumed that all fullerene molecules are charged under photoexcitation and above estimate is physically reasonable. Furthermore, the necessary normalization of the spin carrier concentration in Fig. 4 is not a significant limitation of the model, since the initial photoexcited carrier concentrations at $t=0$ at the three different excitation intensities are linked together by LESR $\approx I_{\mathrm{ex}}^{0.1}$ found in the inset of Fig. 1.

Another prediction of Eq. (4) is that the residual carrier concentration after long times becomes independent of the initial carrier concentration. Plotting all curves from Fig. 4 into one graph, shown in Fig. 6, it appears that the decay curves converge asymptotically. This weak dependence of the long-time residual carrier concentration, i.e., the persistent carrier concentration on the initial carrier concentration was found before.[5] Due to the logarithmic time dependence of the smallest intrapair separation on time, Eq. (2), further confirmation of the convergence of the residual carrier concentration will require much longer times.

The dimensionality $d$ of the conjugated polymer/PCBM composite enters into the derivation of Eq. (4). Here a three-dimensional distribution and interaction of electrons and holes is assumed for the following reasons: First, by nature of the preparation process, the composite deposition results in nonoriented, polymer chains with randomly distributed

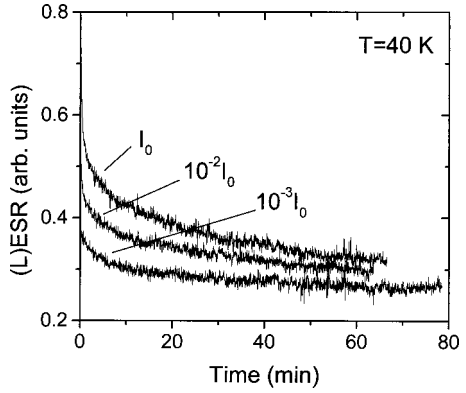


FIG. 6. Decay curves of Fig. 4. The residual carrier densities after long times tend to be independent of the initially photoexcited, carrier densities.

fullerene molecules. Second, it can be assumed that every PCBM molecule is surrounded by and in contact with several polymer chains. The electrons on the PCBM molecules therefore can interact with holes on several polymer chains in all directions, hence leading to a three-dimensional interaction. However, the authors also derived Eq. (1) in one and two dimensions and found that the dimensionality does not affect the decay curves of Fig. 4 for times much longer than $\tau = 6 \times 10^{-5}$ s. Since times $t_1 < 2$ min were already excluded due to geminate recombination, no experimental information can be obtained on the dimensionality. Also the fitting parameter $a^d n_0$, with the dimension $d$, gives no information on the dimensionality of the composite since it appeared physically reasonable in all three dimensions.

The observation of very long-lived carriers in the MDMO-PPV/PCBM composite and in $a$-Si:H as well as the successful explanation of the recombination mechanisms with the same kinetic model is surprising. Although polaronic effects[17] in MDMO-PPV/PCBM are likely to enhance geminate recombination, the recombination kinetics of long-lived carriers in the composite are similar to $a$-Si:H and $a$-Ge:H. In both materials, MDMO-PPV:PCBM and $a$-Si:H, photoexcited carriers recombine rapidly, i.e., approximately exponentially, in the temperature range above about 150–200 K. Also, in both classes of materials the concentrations of the SS-LESR spin carriers are only weakly dependent on the excitation light intensity and a power-law dependence of the SS-LESR spin carriers on excitation intensity $I_{ex}$ according to LESR$\sim I^{\alpha}$ is found. For the MDMO-PPV/PCBM mixture $\alpha$ is approximately 0.1, whereas in $a$-Si:H the exponent was determined to be approximately 0.2.[11,12] This power-law behavior in $a$-Si:H was observed over six orders of magnitude in excitation intensity[11] and recently extended to nine orders.[23] In both materials the long-time recombination kinetics can be well described by tunneling processes, where the lifetime of the long-living photoexcited carriers depends exponentially on the spatial distance that builds up between the carriers that have not recombined.

The very similar recombination behavior of the long-lived carriers in the polymer composite and the inorganic semiconductor strongly indicates that the presented recombination process is common to the two very different types of materials.

## VI. SUMMARY

Persistent photoinduced charge carriers in conjugated polymer/fullerene composites were investigated by LESR. Assuming a model in which the low-temperature recombination rate is strongly dependent on the spatial distance between photoexcited carriers the recombination of persistent, long-living charge carriers can be successfully described. The presented model excludes thermal reexcitation and focuses on tunneling recombination processes of the photoexcited carriers. The long lifetimes are solely ascribed to the large spatial distances that build up among the remaining photoexcited carriers, which have not recombined at a shorter time. The recombination kinetics of long-lived carriers in the composite are similar to those in $a$-Si:H and $a$-Ge:H, for which the model had already been successfully applied,[11] indicating a common recombination mechanism for a subset of photoexcited carriers.

## ACKNOWLEDGMENTS

The authors thank J. C. Hummelen for providing the fullerene PCBM. N. A. S. is greatly indebted to Professor P. C. Taylor for valuable discussions on low-temperature recombination kinetics and acknowledges support by E. E. T. (EETK97115) and CW-NO in the PIONIER program, the Netherlands. This work is supported by the ''Fonds zur Förderung der wissenschaftlichen Forschung'' of Austria (Project No. P-12680-CHE) and was also performed within the Christian Doppler Foundations dedicated to Plastic Solar Cells funded by the Austrian Ministry of Economic Affairs and Quantum Solar Energy Linz GmbH. The authors also gratefully acknowledge the support of the European Community (Joule III).

[1] N. S. Sariciftci, L. Smilowitz, A. J. Heeger, and F. Wudl, Science **258**, 1474 (1992).

[2] S. Morita, A. A. Zakhidov, and K. Zoshino, Solid State Commun. **82**, 249 (1992).

[3] C. J. Brabec, G. Zerza, N. S. Sariciftci, G. Cerullo, S. DeSilvestri, S. Luzzati, and J. C. Hummelen, Chem. Phys. Lett. **340**, 232 (2001).

[4] B. Kraabel, C. H. Lee, D. McBranch, D. Moses, N. S. Sariciftci, and A. J. Heeger, Chem. Phys. Lett. **213**, 389 (1993).

[5] V. Dyakonov, G. Zoriniants, M. Scharber, C. J. Brabec, R. A. J. Janssen, J. C. Hummelen, N. S. Sariciftci, Phys. Rev. B **59**, 8019 (1999).

[6] C. J. Brabec, H. Johansson, A. Cravino, N. S. Sariciftci, D. Comoretto, G. Dellepiane, and I. Moggio, J. Chem. Phys. **111**,

10354 (1999).
[7] J. M. Leng, R. P. Mc Call, K. R. Cromack, J. M. Ginder, H. J. Ye, Y. Sun, S. K. Manohar, A. G. MacDiarmid, and A. J. Epstein, Phys. Rev. B **68**, 1184 (1991).
[8] N. Karl, in *Defect Control in Semiconductors*, edited by K. Sumino (North-Holland, Amsterdam, 1990), Vol. II, p. 1725.
[9] A. Samoc, M. Samoc, and N. Karl, Sci. Pap. Inst. Org. Phys. Chem. of Wroclaw Technical University **16**, 267 (1978).
[10] M. Samoc, A. Samoc, J. Sworakowski, and N. Karl, J. Phys. C **16**, 171 (1983).
[11] B. Yan, N. Schultz, A. L. Efros, and P. C. Taylor, Phys. Rev. Lett. **84**, 4180 (2000).
[12] N. Schultz, Ph.D. thesis, University of Utah, Salt Lake City, Utah, 1999.
[13] J. C. Hummelen, B. W. Knight, F. Lepec, F. Wudl, J. Yao, and C. L. Wilkins, J. Org. Chem. **60**, 532 (1995).
[14] D. J. Dunstan, Physica (Amsterdam) **117B/118B**, 902 (1983).
[15] B. I. Shklovskii, H. Fritzsche, and S. D. Baranovskii, Phys. Rev. Lett. **62**, 2989 (1989).
[16] E. I. Levin, S. Marianer, and B. I. Shklovskii, Phys. Rev. B **45**, 5906 (1992).
[17] S. D. Baranovskii, E. L. Ivchenko, and B. I. Shklovskii, Zh. Eksp. Teor. Fiz. **92**, 2234 (1987) [Sov. Phys. JETP **65**, 1260 (1987)].
[18] S. D. Baranovskii, H. Fritzsche, E. I. Levin, I. M. Ruzin, and B. I. Shklovskii, Zh. Eksp. Teor. Fiz. **96**, 4 (1989) [Sov. Phys. JETP **69**, 773 (1989)].
[19] P. W. M. Blom, M. J. M. de-Jong, and M. G. van-Munster, Phys. Rev. B **55**, 656 (1997).
[20] N. Schultz, B. Yan, A. L. Efros, and P. C. Taylor, J. Non-Cryst. Solids **266–269**, 372 (2000).
[21] R. A. J. Janssen, D. Moses, and N. S. Sariciftci, J. Chem. Phys. **101**, 9519 (1994).
[22] R. A. J. Janssen, J. C. Hummelen, K. H. Lee, K. Pakbaz, N. S. Sariciftci, A. J. Heeger, and F. Wudl, J. Chem. Phys. **103**, 788 (1995).
[23] N. Schultz and P. C. Taylor (unpublished).